THE JOURNAL OF BIOLOGICAL CHEMISTRY VOL. 290, NO. 1, pp. 568–576, January 2, 2015

Na^+ Inhibits the Epithelial Na^+ Channel by Binding to a Site in an Extracellular Acidic Cleft*

Received for publication, August 20, 2014, and in revised form, November 3, 2014 Published, JBC Papers in Press, November 11, 2014, DOI 10.1074/jbc.M114.606152

Ossama B. Kashlan[‡1], **Brandon M. Blobner**[‡], **Zachary Zuzek**[‡], **Michael Tolino**[‡], **and Thomas R. Kleyman**[‡§]

From the Departments of [‡]*Medicine and* [§]*Cell Biology, University of Pittsburgh, Pittsburgh, Pennsylvania 15261*

Background: External Na^+ inhibits ENaC.
Results: Mutations centered about a key aspartate in an acidic cleft weakened Na^+ inhibition and altered inhibitor selectivity.
Conclusion: The acidic cleft hosts an inhibitory Na^+ binding site.
Significance: The acidic cleft harbors a key Na^+ binding site for ENaC and perhaps sites for ligands that regulate other members of the ENaC/degenerin family.

The epithelial Na^+ channel (ENaC) has a key role in the regulation of extracellular fluid volume and blood pressure. ENaC belongs to a family of ion channels that sense the external environment. These channels have large extracellular regions that are thought to interact with environmental cues, such as Na^+, Cl^-, protons, proteases, and shear stress, which modulate gating behavior. We sought to determine the molecular mechanism by which ENaC senses high external Na^+ concentrations, resulting in an inhibition of channel activity. Both our structural model of an ENaC α subunit and the resolved structure of an acid-sensing ion channel (ASIC1) have conserved acidic pockets in the periphery of the extracellular region of the channel. We hypothesized that these acidic pockets host inhibitory allosteric Na^+ binding sites. Through site-directed mutagenesis targeting the acidic pocket, we modified the inhibitory response to external Na^+. Mutations at selected sites altered the cation inhibitory preference to favor Li^+ or K^+ rather than Na^+. Channel activity was reduced in response to restraining movement within this region by cross-linking structures across the acidic pocket. Our results suggest that residues within the acidic pocket form an allosteric effector binding site for Na^+. Our study supports the hypothesis that an acidic cleft is a key ligand binding locus for ENaC and perhaps other members of the ENaC/degenerin family.

The epithelial Na^+ channel (ENaC)[2] is a highly Na^+-selective heterotrimeric channel whose activity is modified by a variety of extracellular factors (1, 2). ENaC-mediated Na^+ conductance through the apical membrane is rate-limiting for transepithelial Na^+ absorption in many Na^+-transporting epithelia (2). In the distal nephron, this transporter has a crucial role in extracellular fluid volume regulation and is under the control of the volume-regulatory hormones aldosterone and vasopressin (2, 3). The role of ENaC in transepithelial Na^+ transport is broad because the channel is expressed in many transporting epithelia, including the distal nephron, lung airway and alveoli, distal colon, sweat glands, lingual epithelia, and inner ear (4–6). ENaC subunits are also expressed in vascular smooth muscle and endothelial cells, where they appear to modulate vascular tone (7).

Sensitivity to extracellular factors is a characteristic of members of the ENaC/degenerin family. For ENaC, a high extracellular [Na^+] inhibits the channel through at least two mechanisms. First, external Na^+ rapidly inhibits ENaC by directly binding to extracellular allosteric effector sites within the channel. This allosteric inhibition, referred to as Na^+ self-inhibition, reflects a low-affinity (tens of micromolar), pH-sensitive, non-voltage-sensitive reduction in ENaC open probability (8–13). This inhibitory effect is also cation-selective because both Na^+ and Li^+ inhibit the channel, whereas K^+ has a modest inhibitory effect at best, and protons activate the channel (9, 10). Second, an elevated intracellular Na^+ concentration inhibits the channel over a slow time course (14, 15).

The extracellular domains of members of the ENaC gene family likely host allosteric effector sites that sense factors in the extracellular environment. For example, acid-sensing ion channels (ASICs) are proton-activated. The resolved structure of ASIC1 features an acidic pocket in each subunit that was proposed to contain proton binding sites competent to trigger gating (16). A major challenge in elucidating ENaC gene family function has been the ability to distinguish ligand binding from downstream transduction steps. The crystal structure of ASIC1 suggests several putative proton binding sites, and mutations at select sites affect acid activation of ASIC1 (17–19). However, one cannot readily distinguish a proton binding site from sites involved in transmitting conformational changes to the channel gate. In this work, we used inhibitor specificity to tackle this challenge.

ENaCs are activated by proteases, which cleave the α and γ subunits at specific sites, releasing imbedded inhibitory tracts (1, 20–23). On the basis of ASIC1 homology and our work that identified the binding site of a peptide derived from the α subunit inhibitory tract, we developed a structural model of the ENaC α subunit (24, 25). We found that the α subunit inhibi-

* This work was supported, in whole or in part by National Institutes of Health Grants R01 DK051391 (to T. R. K.), R01 DK098204 and K01 DK078734 (to O. B. K.), P30 DK079307, and T32 DK061296.
[1] To whom correspondence should be addressed: Dept. of Medicine, University of Pittsburgh, 3550 Terrace St., Pittsburgh, PA. Tel.: 412-628-9081; E-mail: obk2@pitt.edu.
[2] The abbreviations used are: ENaC, epithelial Na^+ channel; ASIC, acid-sensing ion channel 1; P_{Na}, Na^+ permeability; *I-V*, current-voltage; NMDG, *N*-methyl-D-glucamine; P_o, open probability; I_{Peak}, peak current; I_{SS}, steady-state current.

tory tract lies adjacent to an acidic region that is homologous to the ASIC1 acidic cleft. We hypothesized that specific residues within the acidic cleft of the α subunit form a Na^+ binding site required for the Na^+ self-inhibition response.

Na^+ self-inhibition is an allosteric response. Channel modifications that affect the apparent strength of Na^+ self-inhibition could alter channel behavior at different steps in this regulatory process. Experimental manipulations that affect Na^+ self-inhibition could alter the Na^+ binding site, transduction steps subsequent to Na^+ binding, or the stability of the open state relative to the closed state of the channel independent of Na^+ binding. The fact that ENaC is both regulated by external Na^+ and conducts Na^+ complicates our ability to differentiate the Na^+ binding step from other steps in the Na^+ self-inhibition mechanism. To define sites within the channel periphery that participate in Na^+ binding, we studied properties that directly reflect this event. Accordingly, we measured the effect of mutations on the effector or cation specificity of the Na^+ self-inhibition response. Select mutations within the acidic cleft weakened Na^+ self-inhibition and resulted in channels that were more effectively inhibited by Li^+ or K^+ than by Na^+, in contrast to the wild-type channel phenotype, where Na^+ is the most potent inhibitor. We identified a single titratable residue whose mutation abrogated Na^+ self-inhibition as well as channel activation by acidic pH. Through cross-linking, we demonstrate that constraining movements of adjacent structures within the acidic cleft reduced channel activity. Our data show that the acidic cleft of the α subunit of ENaC hosts an allosteric effector binding site for Na^+ and provide strong support for the concept that interactions of external factors with the extracellular region of ENaC have an important role in modulating channel activity.

EXPERIMENTAL PROCEDURES

ENaC Expression and Mutagenesis—Mouse ENaC subunits were mutated and expressed in *Xenopus* oocytes as described previously (26). All mutations were confirmed by direct sequencing.

Current Measurement—Electrophysiological measurements were performed using a GeneClamp 500B voltage clamp amplifier (Axon Instruments, Foster City, CA) and pClamp 10.2 software (Axon Instruments). Oocytes were placed in a 20-μl recording chamber (AutoMate Scientific, Berkeley, CA) with perfusion (3–5 ml/min) controlled by an eight-channel pinch valve system (AutoMate Scientific). For experiments that did not examine the cation specificity of ENaC inhibition, we used a high Na^+ bath solution (110 mM NaCl, 2 mM KCl, 2 mM $CaCl_2$, and 10 mM HEPES (pH 7.4)). We replaced HEPES with MES for lower pH versions of the high-Na^+ bath solution. To make a low-Na^+ bath solution, we replaced NaCl with 109 mM NMDG and 1 mM NaCl. For experiments that examined the cation specificity of ENaC inhibition, we used buffers that included K^+ channel blockers as described previously (9) (100 mM NMDG-Cl, 0.82 mM $MgCl_2$, 0.41 mM $CaCl_2$, 10 mM NMDG-HEPES, 5 mM $BaCl_2$, and 10 mM TEA-Cl for the $NMDG^+$ solution and with 100 mM NaCl, 100 mM LiCl, and 100 mM KCl replacing NMDG-Cl for the Na^+, Li^+, and K^+ solutions, respectively). Amiloride was dissolved in dimethyl sulfoxide at 100 mM and diluted in bath solution to 10 μM for fixed-voltage experiments or 100 μM for voltage ramp experiments.

Current-Voltage Curve Analysis—The comparison of ENaC inhibition by extracellular Na^+, Li^+, and K^+ is complicated by the fact that ENaC is permeable to these cations by a 1.6:1:<0.01 (Li^+:Na^+:K^+) ratio (27). To measure ENaC inhibition by these ions, we determined the relative Na^+ permeability (P_{Na}) in the presence of each ion from the amiloride-sensitive steady-state current-voltage (*I-V*) curves by fitting each curve to the Goldman-Hodgkin-Katz model as described previously (9) with some modifications. When Na^+ was the only permeant ion present, we fit I-V curves to equation 1,

$$I = P_{Na}\frac{EF^2}{RT}\frac{[Na]_i - [Na]_o \exp\left(-\frac{EF}{RT}\right)}{1 - \exp\left(-\frac{EF}{RT}\right)} \quad \text{(Eq. 1)}$$

where E, F, R, T, $[Na]_i$, and $[Na]_o$ are the membrane potential, Faraday constant, gas constant, absolute temperature, intracellular [Na^+], and extracellular [Na^+], respectively. When the bath solution was switched to Li^+, we fit I-V curves to equation 2,

$$I = P_{Na}\frac{EF^2}{RT}\frac{[Na]_i - \frac{P_{Li}}{P_{Na}}[Li]_o \exp\left(-\frac{EF}{RT}\right)}{1 - \exp\left(-\frac{EF}{RT}\right)} \quad \text{(Eq. 2)}$$

where $[Li]_o$ is extracellular [Li^+] and P_{Li}/P_{Na} was assumed to equal 1.6 on the basis of the ion selectivity of the pore (9, 27). We assumed that the mutations examined here, far from the pore, did not affect the value of P_{Li}/P_{Na}. We also assumed that $[Na]_i$ remained constant throughout the experiment and that intracellular [Li^+] was zero. To minimize changes in $[Na]_i$ during the experiment, we clamped oocytes at −20 mV between voltage ramps. We collected five amiloride-sensitive I-V curves for each oocyte, each using bath solutions with different cations ($NMDG^+$, Na^+, Li^+, K^+, and $NMDG^+$ again) for 1 min, followed by the same solution supplemented with 100 μM amiloride for 20 s. We fit the I-V curves from each oocyte simultaneously using a global fitting routine and Igor Pro 6 (Wavemetrics, Oswego, OR). This allowed us to use data under all conditions to determine a global value for $[Na]_i$ while independently determining local values for P_{Na} under each condition. We assigned values for the global parameters F, R, and T and the local parameters $[Na]_o$ or $[Li]_o \cdot P_{Li}/P_{Na}$. E was the independent variable. Each fit produced five P_{Na} values, one for each condition. We normalized each P_{Na} value to a corrected P_{Na} determined with bath $NMDG^+$ at the beginning and end of the experiment to account for channel rundown, which we assumed was linear over the course of the experiment.

Statistical Analyses—Values presented are mean ± S.E. We performed multiple group comparisons using analysis of variance followed by Tukey post hoc test. We adjusted the significance threshold from $p = 0.05$ for multiple comparisons using the Bonferroni correction. We performed pairwise compari-

sons using Student's *t* test. We considered *p* values of less than 0.05 significant.

RESULTS

Protons Activate Mouse ENaC—Collier and Snyder (10) and Collier *et al.* (28) reported previously that human ENaC is activated by extracellular acidification with an apparent pH_{50} of activation of 6.5. They found that rat ENaC was also activated by acid but at a lower pH (28). Because acidification was associated with reduced Na^+ self-inhibition, they suggested that extracellular acidification activated ENaC by relieving Na^+ self-inhibition. We examined the effect of extracellular acidification on mouse ENaC expressed in *Xenopus* oocytes by two-electrode voltage clamp (Fig. 1*A*). Although modest acidification (to pH 6.5) did not alter channel activity (see below), lowering the extracellular pH from 7.4 to 4.7 stimulated currents by 44 ± 3% ($n = 6$, $p < 0.05$ using paired Student's *t* test). This is similar to the increase observed for human ENaC by lowering the pH from 7.4 to 6.5 (10). When currents are measured under voltage clamp conditions, currents decay over time. We found that the rate of decay of ENaC currents increased from 3.4 ± 0.9%/min to 10.3 ± 0.5%/min with acidification to pH 4.7 ($p < 0.05$ using paired Student's *t* test). Channel activation by reducing extracellular pH to the range that should titrate acidic residues suggested that residues in the acidic cleft could be involved in Na^+ sensing.

Mutation of Sites in the Acidic Cleft Affect Na$^+$ Self-inhibition—Our model of the α subunit features an acidic region at the juncture of the finger, β-ball, and thumb domains (Fig. 1*C*), which has the appearance of an acidic cleft (24). A homologous region in ASIC1 has been proposed to play a role in proton sensing (16). We hypothesized that residues in the vicinity of the acidic cleft of ENaC subunits coordinate Na^+, the first step in the Na^+ self-inhibition response.

To examine whether mutations of residues in the acidic cleft weakened Na^+ self-inhibition, we performed a Trp mutagenesis screen of acidic cleft Asp and Glu residues (Fig. 1*C*, *red spheres*) and measured the effect of mutation on Na^+ self-inhibition. Wild-type or mutant ENaCs were expressed in *Xenopus laevis* oocytes, and ENaC currents were measured by two-electrode voltage clamp. Because ENaC Na^+ self-inhibition manifests slowly relative to bath solution exchange, acutely raising the bath [Na^+] from a low concentration (where the channel open probability (P_o) is high) results in a peak inward current that subsequently declines (8, 11), reflecting Na^+ binding events at extracellular allosteric site(s) that are transduced to reduce channel P_o (*i.e.* Na^+ self-inhibition) (Fig. 1*B*) (12, 13, 29). Of the acidic sites tested, we found that the Trp mutation at αAsp-176, αGlu-362, and αAsp-365 reduced Na^+ self-inhibition (Fig. 1*E*, *red columns*). The latter two lie at the beginning of a loop connecting the sixth and seventh β strands (Fig. 1*C*; *β6-β7 loop*), whereas αAsp-176 on the α1 helix interacts with the β6-β7 loop (Fig. 2*A*).

We hypothesized that β6-β7 loop residues participate in Na^+ binding. We performed Trp scanning mutagenesis of the residues lining the β6-β7 loop and determined the effects of individual mutations on Na^+ self-inhibition (Fig. 1*E*). In our model, the β6-β7 loop extends from the β-ball toward helix α1 of the finger domain, with αLeu-369 at the apex of the loop interacting with αAsp-176 from helix α1 of the finger domain (Figs. 1*C* and 2*A*). We found that a Trp mutation at multiple residues flanking αLeu-369 reduced Na^+ self-inhibition, whereas αL369W enhanced Na^+ self-inhibition.

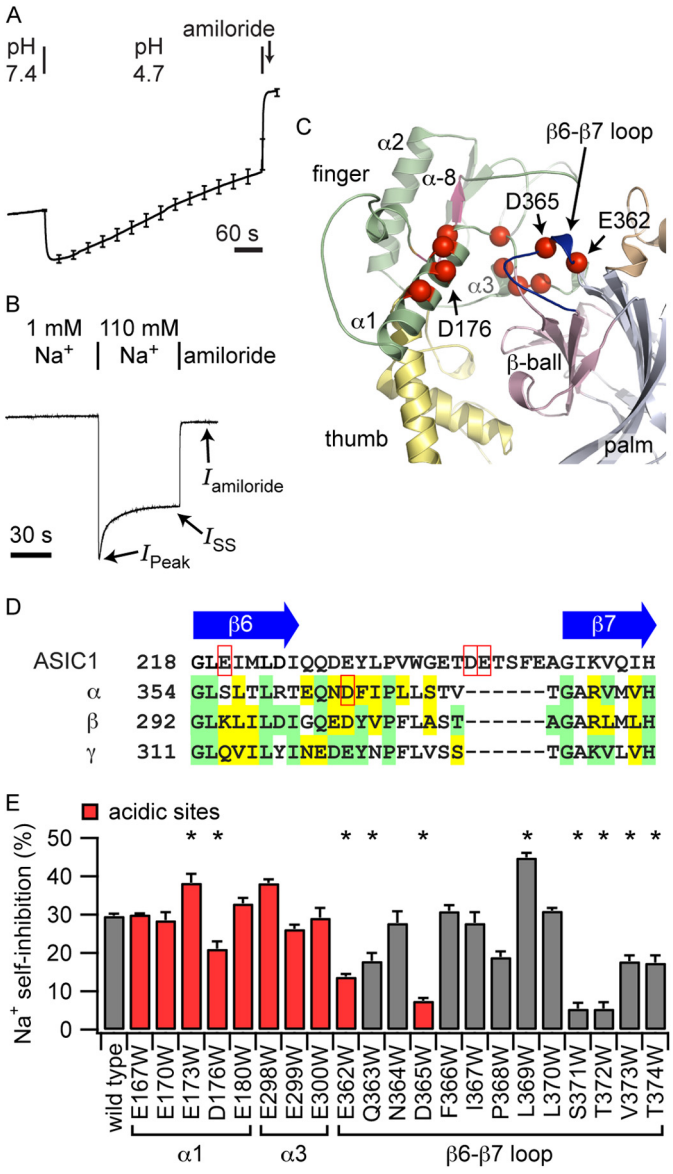

FIGURE 1. **Mutations of acidic cleft residues affect Na$^+$ self-inhibition.** *A*, acidification activates mouse ENaC. Recordings were normalized to the average current prior to acidification. The average of six normalized current tracings is shown, with periodic *error bars* indicating the mean ± S.E. The average starting current was 1.8 ± 0.4 μA. *B*, representative recording of the Na^+ self-inhibition response of wild-type mouse ENaC (−100 mV holding potential). Bathing solutions and the addition of amiloride (10 μM) are noted. I_{Peak} and I_{SS} currents following the transition to a high [Na^+] solution are also noted. *C*, model of the acidic cleft. Acidic residues (*red spheres*) and the β6-β7 loop (*blue*) are highlighted. An imbedded inhibitory tract from which an inhibitory peptide can be derived (*α-8*, *pink*) is located near the acidic cleft. *D*, sequence alignment of the β6-β7 loop region. αAsp-365 and ASIC1 residues implicated in the response to H^+ are highlighted (*red boxes*). *E*, Na^+ self-inhibition of the Trp mutants is reported as $100 \times [1 - (I_{SS} - I_{amiloride})/(I_{Peak} - I_{amiloride})]$. Trp mutation at sites flanking αLeu-369 strongly reduced Na^+ self-inhibition, including at acidic residue αAsp-365. *, $p < 0.002$ *versus* the wild type (n = 6–15 for mutants and 115 for the wild type). Model positions of mutations are noted.

If Na^+ binding to residues in the $\beta6$-$\beta7$ loop results in a decrease in channel activity, then the conformation of the $\beta6$-$\beta7$ loop must be linked to the conformation of the channel gate. It follows that constraining movement of the loop should alter channel activity. We used a cross-linking approach to test this hypothesis. Our model suggested that αLeu-369 at the apex of the $\beta6$-$\beta7$ loop interacts with αAsp-176 from helix $\alpha1$ of the finger domain (Fig. 2*A*). We introduced Cys at αLeu-369 in the $\beta6$-$\beta7$ loop and, simultaneously, to αAsp-176 in helix $\alpha1$ of the finger domain. Because αL369C and αD176C are predicted to be in close proximity, we examined whether these introduced Cys residues formed a natural disulfide bond, linking the $\beta6$-$\beta7$ loop with the $\alpha1$ helix. DTT addition activated ENaC-bearing Cys residues at both sites (Fig. 2, *B* and *C*). This activation required the presence of both introduced Cys residues because DTT did not affect the wild type or channels with a single Cys substitution. The DTT-treated double mutant had modestly reduced Na^+ self-inhibition compared with DTT-treated wild-type channels (22.8 ± 0.5% *versus* 38 ± 2%, $n = 4$, $p < 0.05$), suggesting that the introduced cysteines residues, *per se*, modestly altered channel function. These data suggest that conformational changes that involve the $\beta6$-$\beta7$ loop affect channel activity.

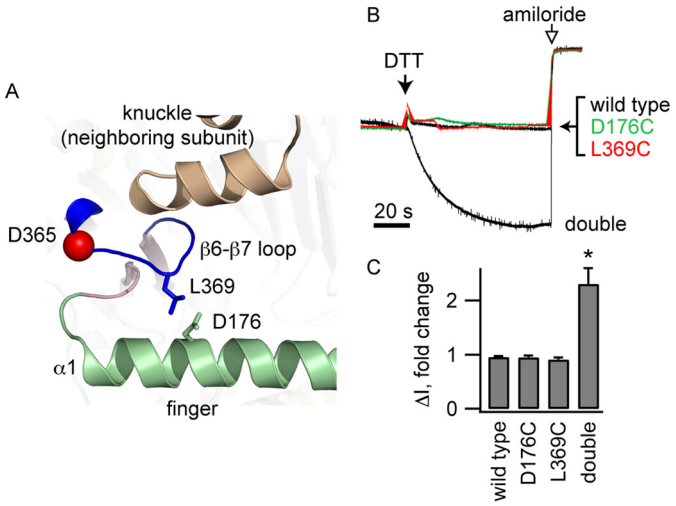

FIGURE 2. **Cross-linking the $\beta6$-$\beta7$ loop to the $\alpha1$ helix reduces channel activity.** *A*, Leu-369 on the $\beta6$-$\beta7$ loop and Asp-176 on helix $\alpha1$ are adjacent in our model of the α subunit. *B*, oocytes expressing wild type ENaC, either of the α subunit single mutants (αD176C or αL369C) or the αD176C/L369C double mutant, were exposed to 10 mM DTT and then amiloride (10 μM) while currents were measured at a holding potential of −100 mV. Representative recordings are shown. Currents were normalized to the current immediately prior to DTT addition. Average currents prior to DTT were −1.7 ± 0.4 μA (wild type), −1.5 ± 0.3 μA (αD176C), −1.9 ± 0.4 μA (αL369C), and −1.1 ± 0.2 μA (αD176C/L369C). *C*, amiloride-sensitive currents following DTT addition normalized to currents prior to DTT ($n = 7$–10). *, $p < 0.01$.

Residues in the Acidic Cleft Determine the Cation Specificity of Inhibition—To identify residues involved in the Na^+ binding step, we measured the effect of specific mutations on the ligand specificity of Na^+ self-inhibition. As noted above, mutations that alter the Na^+ self-inhibition response could reflect changes in the Na^+ binding step, transduction steps subsequent to Na^+ binding, or the relative stability of the open

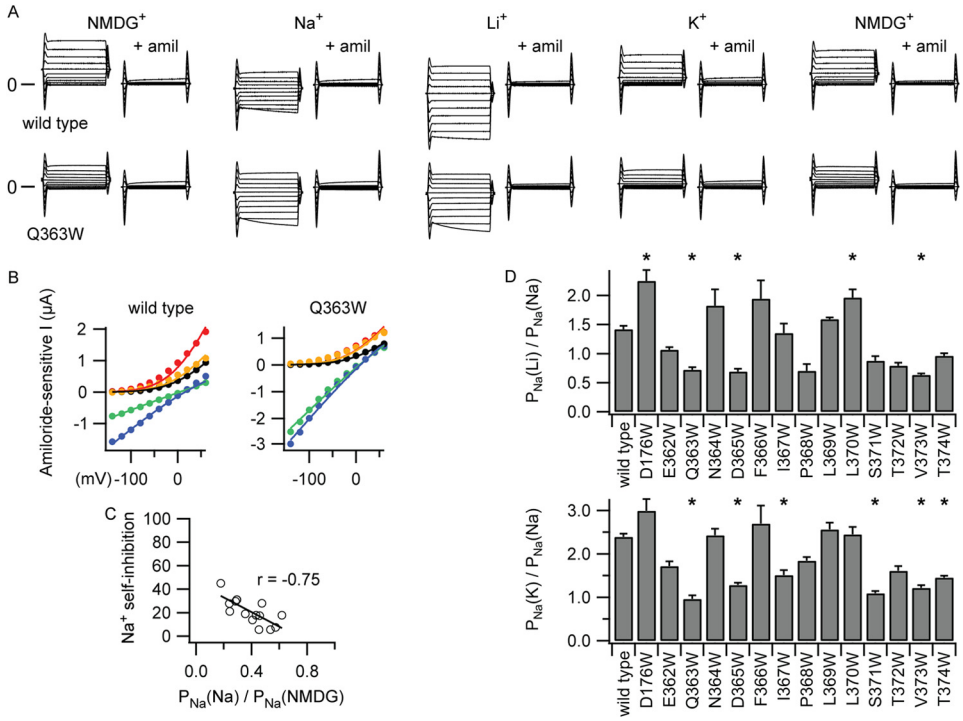

FIGURE 3. **Mutations in the acidic cleft alter the cation selectivity of ENaC inhibition.** *A*, ENaC expressing oocytes were perfused for 1 min with each solution, after which currents were determined at varying holding potentials (−140 to 60 mV in 20-mV steps, 0.5 s/step). Amiloride (*amil*)-supplemented solutions were then perfused for 20 s, followed by measurement of currents at the different holding potentials. *B*, resultant I-V curves were fit with equation 1 or 2 to derive P_{Na} values in each solution (*red*, initial $NMDG^+$; *green*, Na^+; *blue*, Li^+; *black*, K^+; orange, final $NMDG^+$). Measurements in $NMDG^+$ were taken at the beginning and end of each experiment to estimate channel rundown (~2–7%/min), which was used to adjust P_{Na} values for channel rundown. *C*, correlation between Na^+ self-inhibition measured under a constant voltage clamp (Fig. 1*B*) and the ratio of Na^+ permeabilities in Na^+ and $NMDG^+$. *D*, ratio of Na^+ permeabilities measured in different bath solutions: Li^+ *versus* Na^+ (*top panel*) and K^+ *versus* Na^+ (*bottom panel*). *, $p < 0.003$ *versus* wild type ($n = 40$ for the wild type and 5–12 for mutants).

and/or closed states. We reasoned that the ability to discriminate Na^+ and Li^+ from other cations reflects ligand binding.

To compare the inhibition of ENaC by Na^+, Li^+, and K^+, we examined steady-state Na^+ permeability in the presence of different extracellular cations using a method adapted from Bize and Horisberger (9). Amiloride sensitive I-V curves were obtained at steady state in oocytes sequentially perfused with buffers containing $NMDG^+$, Na^+, Li^+, K^+, and then $NMDG^+$ again as the predominant cation (Figs. 3, *A* and *B*). We then fit the I-V curves to equations derived from the Goldman-Hodgkin-Katz model of ion flux to determine the relative permeability of ENaC to Na^+ (P_{Na}) under each condition (Fig. 3*B* and equations 1 and 2, see "Experimental Procedures"). Reductions in P_{Na} in Na^+, Li^+, or K^+ relative to P_{Na} in $NMDG^+$ reflect ENaC inhibition by these effectors. We assumed that the Li^+/Na^+ permeability ratio (P_{Li}/P_{Na}, *i.e.* the pore selectivity) is 1.6 on the basis of published reports (27, 30) and is not affected by these mutations far from the pore. We assumed that the K^+ permeability is 0. We also assumed that intracellular [Na^+] ($[Na]_i$) remains steady through the course of the experiment. With these assumptions, fitting each curve to the Goldman-Hodgkin-Katz model depends on two variables, P_{Na} and $[Na]_i$, which have little interdependency for curve fitting purposes (Fig. 3*B*). We corrected for channel rundown using P_{Na} measurements in $NMDG^+$ at the beginning and end of the experiment and assuming a linear rundown.

The extent of Na^+ inhibition measured by this method correlated with Na^+ self-inhibition measured by rapidly switching solutions from $NMDG^+$ to Na^+ (Fig. 1*B*). Na^+ self-inhibition is given by the ratio of P_{Na} with extracellular Na^+ to P_{Na} with extracellular $NMDG^+$ ($P_{Na}(Na)/P_{Na}(NMDG)$). We plotted the results for the wild type, αD176W, and the β6-β7 loop Trp mutants (Fig. 3*C*). The fitted line gave a Pearson's correlation coefficient of −0.75 ($p < 0.005$). Notably, the fitted line is shifted from its theoretical position (the diagonal from (0, 100) to (1, 0)) toward the origin. This may reflect, in part, an underestimation of the peak current (*e.g.* Fig. 1*B*), which depends upon the efficiency of solution exchange and the kinetics of channel inhibition.

Wild-type mouse ENaC showed a slightly different effector specificity for channel inhibition ($Na^+ > Li^+ \gg K^+$, Fig. 3*D*) than what has been reported for human ENaC ($Na^+ \approx Li^+ > K^+$) (9). Trp substitutions at sites toward the beginning or end of the β6-β7 loop changed this order. For αQ363W, αD365W, and αV373W, Li^+ was a more potent inhibitor than Na^+, whereas K^+ and Na^+ had similar inhibitory effects. The mutants αI367W, αS371W, and αT374W exhibited weakened Na^+ inhibition relative to K^+, whereas αL370W exhibited weakened Li^+ inhibition relative to Na^+. Trp mutation at other sites neighboring αGln-363 and αVal-373 showed trends toward changing inhibitor specificity but were not significantly different from the wild type.

To corroborate these results, we measured effector specificity using a second method that adapted a fixed-voltage protocol for measuring Na^+ self-inhibition (Fig. 1*B*). First we examined Na^+ inhibition by rapidly switching from an $NMDG^+$ solution to a Na^+ solution while voltage-clamping the oocyte at −100 mV (Fig. 4). As described above, this leads to a rapid inward

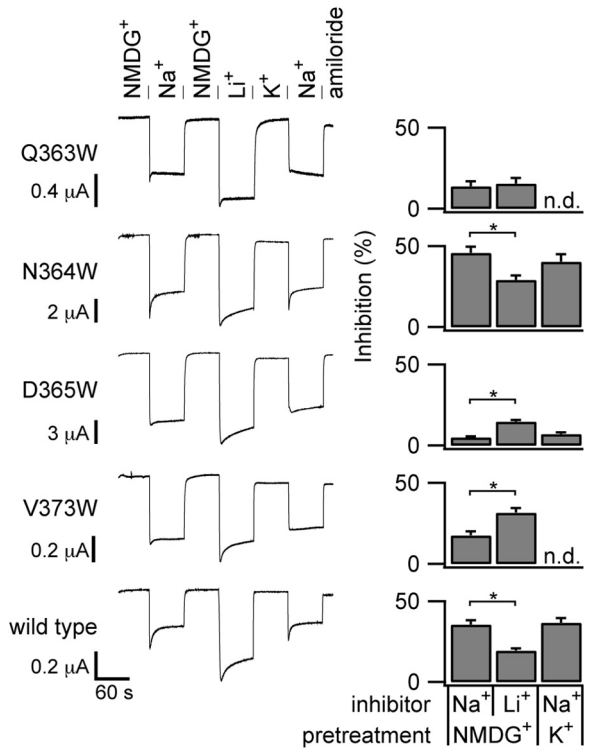

FIGURE 4. **Cation specificity of the inhibitory response measured with a constant voltage clamp.** ENaC-expressing oocytes were voltage-clamped at −100 mV during current measurements. Perfusates with 100 mM of the indicated cation were switched every 60 s. Amiloride was added to the Na^+ solution at the end of each experiment. Inhibition upon Na^+ or Li^+ addition was calculated as in Fig. 1*E*. Quantified results are from 18 wild-type experiments and six to nine experiments for each mutant. *, $p < 0.05$ by paired Student's *t* test. *n.d.,* not determined.

peak current (I_{Peak}) that declines to a steady-state level (I_{SS}). The fall from I_{Peak} to I_{SS} reflects Na^+ self-inhibition. Because ENaC also conducts Li^+, we measured Li^+ inhibition in a similar manner by rapidly switching from an $NMDG^+$ solution to a Li^+ solution. Because ENaC does not appreciably conduct K^+, we measured K^+ inhibition indirectly by examining the effect of K^+ pretreatment on Na^+ inhibition. Instead of initially bathing the oocyte in an $NMDG^+$ solution, where ENaC P_o is high (12), we used a K^+ solution. If channel inhibition by K^+ is much weaker than by Na^+, switching from $NMDG^+$ or K^+ to Na^+ should produce similar Na^+ self-inhibition responses. This is what we observed for wild-type channels (Fig. 4). If channel inhibition by K^+ and Na^+ are similar, then pretreatment with K^+ should attenuate the inhibitory response to Na^+, as we observed with the αV373W and αD365W mutants (Fig. 4). If K^+ inhibits an ENaC mutant more effectively than Na^+, then switching from a K^+ to an Na^+ bath should induce a rise in current that represents Na^+ relief of K^+ inhibition. This was seen with the αQ363W mutant (Fig. 4). Using this fixed-voltage protocol, we also found that Na^+ was a more effective inhibitor than Li^+ of wild-type mouse ENaC. αN364W exhibited a pattern similar to the wild type. For αV373W and αD365W, this pattern was reversed. For αQ363W, Li^+ and Na^+ were similarly effective inhibitors. For the wild type and αN364W, K^+ pretreatment did not alter Na^+ self-inhibition when compared with $NMDG^+$ pretreatment.

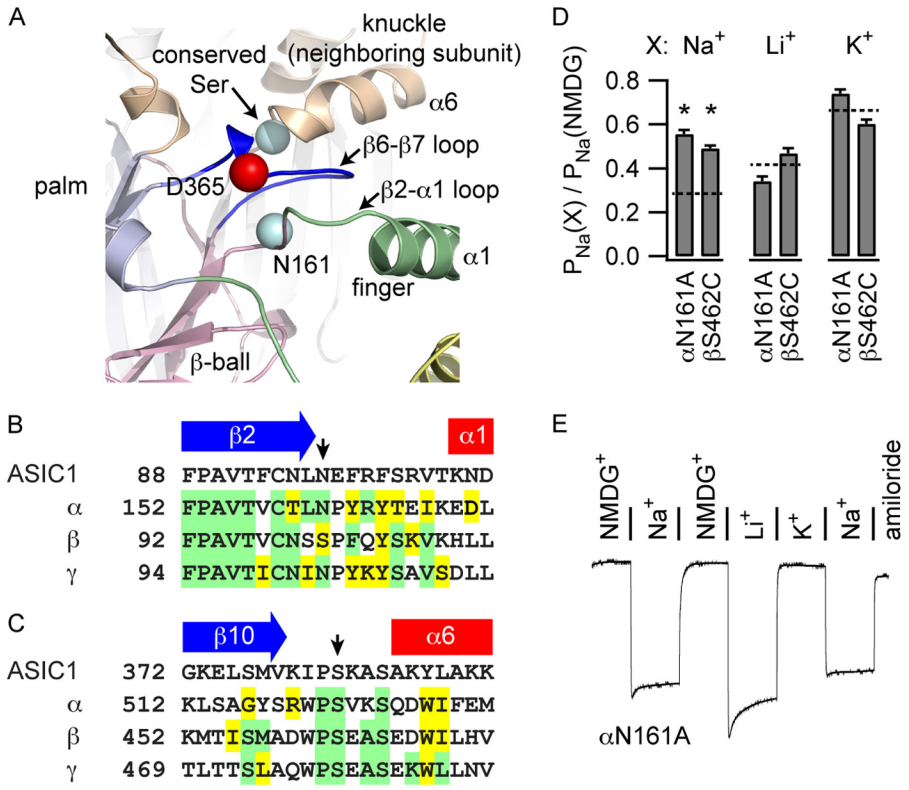

FIGURE 5. **Specific conserved sites on structures near αD365 weaken Na^+ inhibition.** *A*, structures near the β6-β7 loop in an ENaC α trimer model, including the β2-α1 loop of the α subunit and the beginning of helix α6 of the neighboring β subunit. *B* and *C*, sequence alignments of the β2-α1 loop (*B*) and the β10-α6 loop (*C*), with sites of interest indicated by *arrows*. *D*, P_{Na} in various bath solutions (*X*) was determined as described for Fig. 3. P_{Na} values where Na^+, Li^+, or K^+ were the predominant cation were normalized to P_{Na} determined in $NMDG^+$. *, $p < 0.003$ *versus* wild ($n = 40$ for the wild type and 8 for mutants). Values for the wild type are indicated by *dashed lines*. *E*, representative experiment examining the effector specificity of inhibition of αN161A under a constant voltage clamp. Quantification of eight experiments gave values of 10.9 ± 0.9% for Na^+ inhibition following $NMDG^+$ pretreatment, 25 ± 1% for Li^+ inhibition, and 7 ± 1% for Na^+ inhibition following K^+ pretreatment. Comparable wild type values were 36 ± 3%, 19 ± 2%, and 34 ± 3%, respectively ($n = 6$). Na^+ inhibition measurements following $NMDG^+$ or K^+ perfusion was weaker in both cases for αN161A compared with the wild type ($p < 0.05$, Student's *t* test). K^+ pretreatment did not affect Na^+ inhibition of either the wild type or αN161A compared with $NMDG^+$ pretreatment (p = not significant, paired Student's *t* test). In contrast to the wild type, Li^+ inhibition was greater than Na^+ inhibition for αN161A channels ($p < 0.05$, paired Student's *t* test).

Sites Adjacent to the β6-β7 Loop Affect Inhibitor Specificity—Mutations in the β6-β7 loop affect the cation selectivity of channel inhibition. Our model of a hypothetical ENaC α trimer suggested that adjacent sites could coordinate a bound ion in concert with sites in the β6-β7 loop (Fig. 5*A*). αAsn-161 is at the end of a highly conserved sequence in the β2-α1 loop connecting the β ball and the finger domain in the α subunit and lies in proximity to the β6-β7 loop (Fig. 5*B*). The first Ser within a WPS*XX*S motif in the knuckle domain of a neighboring subunit lies across the plane of the α subunit β6-β7 loop (Fig. 5*C*). According to recent reports, the neighboring knuckle domain is part of the β subunit (31, 32). Notably, a polymorphism of the Trp residue in the WPS*XX*S motif of the human α subunit (αW493R) was associated with a loss of Na^+ self-inhibition and an increased channel P_o (33). We mutated αAsn-161 to Ala and βSer-462 to Cys and assessed the resultant inhibitor specificity. We compared P_{Na} values derived from steady state I-V curves using different perfusion buffers as described above. Both αN161A and βS462C weakened Na^+ inhibition but did not affect Li^+ or K^+ inhibition (Fig. 5*D*). We corroborated these results for αN161A using the fixed-voltage protocol for measuring self-inhibition induced by Na^+ or Li^+ (Fig. 5*E*), which showed a pattern of inhibition similar to αD365W and αV373W and different from wild-type ENaC (Fig. 4).

Protonation of αAsp-365 Activates ENaC—Acidification of the extracellular solution increased mouse ENaC currents (Fig. 1*A*). We hypothesized that protonation of a Na^+-coordinating residue weakens Na^+ binding, diminishing Na^+ self-inhibition and activating the channel. To identify titratable residues responsible for this activation, we performed titrations of wild-type channels and three mutants: αD176W, αE362W, and αD365W (Fig. 6*B*). We performed each experiment as described for Fig. 1*A* and measured the acute amiloride-sensitive change in current upon acidification from pH 7.4. Although each mutant blunts Na^+ self-inhibition (Fig. 1), we observed that only αD365W reversed the effect of acidification on ENaC currents, causing currents to modestly fall instead of rise (Figs. 1*A* and 6, *A* and *B*). Channels bearing αD176W or αE362W responded to acidification similarly to wild-type. For all groups tested, effects at pH 5.5 were intermediate to effects at pH 4.7. In contrast to human ENaC (10), effects at pH 6.5 were minor for all groups tested.

We also examined the effect of acidification on the Na^+ self-inhibition response. At pH 4.7, the wild type and the three Trp mutants exhibited low Na^+ self-inhibition responses (Fig. 6, *C* and *D*). These data, taken together, suggest that reducing the pH to 4.7 or altering the Asp group at αAsp-365 removes an important coordinating group from one of the putative Na^+

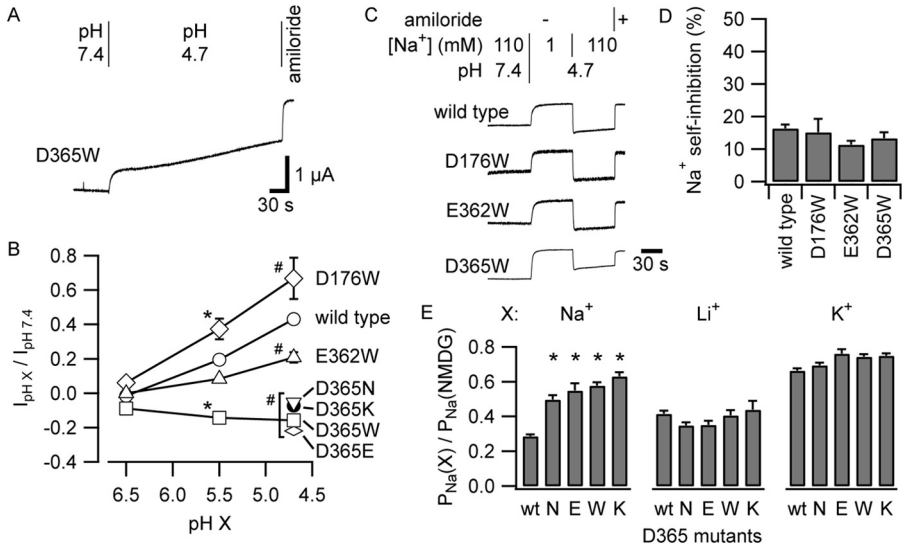

FIGURE 6. **αAsp-365 mutants lack acid-dependent channel activation.** *A*, acidification inhibits αD365W currents. *B*, effects of pH titration on the wild type and select mutants of acidic residues in the acidic cleft. Each experiment was performed as in Figs. 1*A* and 6*A* while varying the final pH. The acute amiloride-sensitive change in current upon acidification to pH 6.5, 5.5, or 4.7 was quantified. For experiments in which currents increased as a result of acidification, we used the maximal increase in current, which occurred at 10 ± 1 s after initiating solution exchange (Fig. 1*A*). For experiments in which the current decreased as a result of acidification, there was no transient nadir because both the fast and slow phases of the change affected the current in the same direction (*A*). For quantification of the acute effect of changing pH on current, we used the current value at 10 s after initiating solution exchange. *, $p < 0.01$ *versus* the wild type at pH 5.5; #, $p < 0.005$ *versus* the wild type at pH 4.7. For all groups, $n = 5–8$. *C*, acidification weakens Na^+ self-inhibition. Shown are representative current recordings of oocytes expressing the wild type or α subunit mutants and voltage-clamped at −100 mV. Solutions were exchanged rapidly as indicated. *D*, Na^+ self-inhibition was quantified at pH 4.7 as for Fig. 1*E*. No significant differences were detected ($n = 5–8$). *E*, experiments were performed as described for Fig. 3. P_{Na} values where Na^+, Li^+, or K^+ were the principal cation were normalized to P_{Na} determined in $NMDG^+$. *, $p < 0.003$ *versus* the wild type ($n = 40$ for the wild type and 5–8 for mutants).

binding sites of ENaC. To further address this hypothesis, we examined the response of the channel to acidification after introducing conservative Glu or Asn substitutions at αAsp-365 or after reversing the charge by Lys substitution. All three αAsp-365 mutants (Glu, Asn, and Lys) prevented channel activation by acidification, echoing our result with αD365W (Fig. 6*B*). We also examined the effect of these mutations on Na^+, Li^+, or K^+ inhibition at steady state using the voltage ramp method (Fig. 3). We found that each mutant specifically weakened Na^+ inhibition (Fig. 6*E*). Our data suggest that the specific moiety at position α365, rather than charge *per se*, is needed to confer "full" sensitivity to external Na^+.

DISCUSSION

ENaCs are members of a family of ion channels that respond to factors in the extracellular environment. One of the external factors that regulate ENaC is Na^+. There are multiple lines of evidence supporting the notion that Na^+ binding to one or more effector sites within the extracellular domains results in the inhibition of channel activity in an allosteric manner (1, 12, 13, 29, 34). Given that allosteric transitions are required for this process, it is not surprising that many substitutions throughout the extracellular regions of ENaC subunits altered the Na^+ self-inhibition response. For example, we and others have reported mutations that weaken Na^+ self-inhibition in the palm domain, thumb domain, β ball-thumb domain interface, knuckle domain, finger domain, and subunit interfaces and among the Cys involved in disulfide bridges (13, 25, 28, 31, 33, 35–39). Furthermore, it is not surprising that mutations in transmembrane helical residues that interfere with pore closure and increase channel P_o (*e.g.* βS518K) significantly weaken Na^+ self-inhibition (38, 40). Likewise, other maneuvers that increase channel P_o, *e.g.* Zn^{2+} addition (41) or Cl^- removal (42), weaken apparent Na^+ self-inhibition. In summary, on the basis of previous studies, it has been difficult to discern whether specific mutations that change Na^+ self-inhibition do so by altering Na^+ binding, downstream transduction steps, or the baseline stability of the open or closed states of the channel.

We postulated that Na^+ binds to a site defined, in part, by acidic residues, consistent with Na^+-bound protein structures (43, 44) and the predominance of oxygen atoms coordinating Na^+ in model small molecules (45). We also reasoned that the preference of the channel for Na^+ over other cations as an inhibitory effector originates from the binding site(s) rather than from subsequent transduction steps. On these premises, we tested the ability of α subunit acidic cleft mutants to both affect Na^+ self-inhibition and alter the relative inhibitory efficacy of Na^+, Li^+, and K^+. Mutation of αAsp-365 or neighboring residues in our α subunit model weakened inhibition by external Na^+ and altered the cation selectivity of channel inhibition. Even conservative αAsp-365 mutations (Glu or Asn) had this effect. αAsp-365 substitutions also prevented channel activation by acidification regardless of whether a conservative or non-conservative substitution was used. These results support the notion that αAsp-365 has a role in Na^+ binding and the subsequent reduction in channel P_o, and that acidification activates ENaC by protonating αAsp-365 and disrupting Na^+ binding at an effector site that includes αAsp-365.

Our results also suggest that there are multiple effector sites for Na^+ self-inhibition. All mutants tested at or near αAsp-365 retained at least a small Na^+ self-inhibition response. Acidifi-

cation had no effect on the Na^+ self-inhibition response of αD365W, but reduced the response of the wild type and other mutants to similarly low but measurable values (compare Figs. 1*E* and 6*D*). We propose that there are additional Na^+ effector sites. Because αD365W has a small but measurable Na^+ self-inhibition response, at least one of the additional effector sites does not depend on residues titratable in the pH 7.4–4.7 range. Accordingly, conservative mutations of the β and γ sites that correspond to αAsp-365 (βD302N and γE322Q) exhibited Na^+ self-inhibition similar to the wild type (βD302N, 33 ± 4%; γE322Q, 27 ± 3%; wild type, 32 ± 2%; n = 5–6; p = not significant).

Other members of the ENaC/Deg family have an Asp or Glu residue at the position equivalent to mouse αAsp-365 (*e.g.* Glu-229 in chicken ASIC1, Fig. 1*D*). This residue lies at the beginning of the β6-β7 loop, which connects the β-ball and palm domains (1, 16). Electrostatic calculations for the ASIC1 Glu (equivalent to αAsp-365) predicted a pK_a of 7.4, a prerequisite for proton sensing in the physiological range (17). However, mutating this residue in ASIC1 to Gln had little effect on the pH sensitivity of channel activation (17, 18). The δ subunit of ENaC replaces the α subunit in the channel complex expressed in some tissues of several species, including humans (but not rodents). Interestingly, human δβγ channels are poorly inhibited by external Na^+ (46). The δ subunit has a Pro residue at the equivalent site to αAsp-365. However, mutating δPro-314 to Asp did not sensitize human δβγ ENaC to external Na^+ (data not shown). This observation suggests that there are residues in addition to αAsp-365 that are needed to form a Na^+ binding site in the α subunit.

The β6-β7 loop of ASIC1 interacts with the finger and thumb domains and is six residues longer than its ENaC subunit counterparts (Fig. 1*D*). In our α subunit model, the shorter β6-β7 loop approaches the α1 helix in the finger domain but does not abut thumb domain residues (Fig. 1*C*) (24). Our results demonstrating that αD176C in the α1 helix and αL369C in the β6-β7 loop form a disulfide bond suggest that these structures are indeed in close proximity and that stabilizing interactions between the α1 helix and the β6-β7 loop is inhibitory. The ASIC1 β6-β7 loop includes Asp-238 and Glu-239 (cASIC1 numbering, Fig. 1*D*) that pair with thumb domain residues Asp-350 and Asp-346, respectively. These thumb domain residues have been proposed to sense protons (16). Krauson *et al.* (19) showed that mutating Asp-346 in mouse ASIC1a results in a biphasic pH activation curve, suggesting that this mutation specifically weakened of one of multiple proton sensing sites. ASIC1 residues Asp-238 and Glu-239 and ENaC residues α371–373 are located in a similar region of the β6-β7 loop (Fig. 1*D*), where α subunit Trp substitutions weaken Na^+ self-inhibition and alter the cation selectivity of this process (Figs. 1, 3, and 4). Baconguis and Gouaux (47) provided additional evidence for the role of the β6-β7 loop in modulating channel gating in response to external factors. They found that psalmotoxin, an ASIC1 inhibitor, extends an Arg-rich hairpin into the acidic pocket and forms hydrogen bonds with the β6-β7 loop backbone (47). These previous observations and our current findings, taken together, suggest that the β6-β7 loop has evolved within members of the ENaC/degenerin family members to facilitate the sensing of specific factors.

REFERENCES

1. Kashlan, O. B., and Kleyman, T. R. (2011) ENaC structure and function in the wake of a resolved structure of a family member. *Am. J. Physiol. Renal Physiol.* **301,** F684–F696
2. Bhalla, V., and Hallows, K. R. (2008) Mechanisms of ENaC regulation and clinical implications. *J. Am. Soc. Nephrol.* **19,** 1845–1854
3. Pearce, D., Soundararajan, R., Trimpert, C., Kashlan, O. B., Deen, P. M., and Kohan, D. E. (2014) Collecting duct principal cell transport processes and their regulation. *Clin. J. Am. Soc. Nephrol.* in press
4. Duc, C., Farman, N., Canessa, C. M., Bonvalet, J. P., and Rossier, B. C. (1994) Cell-specific expression of epithelial sodium channel α, β, and γ subunits in aldosterone-responsive epithelia from the rat: localization by *in situ* hybridization and immunocytochemistry. *J. Cell Biol.* **127,** 1907–1921
5. Kretz, O., Barbry, P., Bock, R., and Lindemann, B. (1999) Differential expression of RNA and protein of the three pore-forming subunits of the amiloride-sensitive epithelial sodium channel in taste buds of the rat. *J. Histochem. Cytochem.* **47,** 51–64
6. Gründer, S., Müller, A., and Ruppersberg, J. P. (2001) Developmental and cellular expression pattern of epithelial sodium channel α, β, and γ subunits in the inner ear of the rat. *Eur. J. Neurosci.* **13,** 641–648
7. Drummond, H. A., Gebremedhin, D., and Harder, D. R. (2004) Degenerin/epithelial Na^+ channel proteins: components of a vascular mechanosensor. *Hypertension* **44,** 643–648
8. Fuchs, W., Larsen, E. H., and Lindemann, B. (1977) Current-voltage curve of sodium channels and concentration dependence of sodium permeability in frog skin. *J. Physiol.* **267,** 137–166
9. Bize, V., and Horisberger, J. D. (2007) Sodium self-inhibition of human epithelial sodium channel: selectivity and affinity of the extracellular sodium sensing site. *Am. J. Physiol. Renal Physiol.* **293,** F1137–F1146
10. Collier, D. M., and Snyder, P. M. (2009) Extracellular protons regulate human ENaC by modulating Na^+ self-inhibition. *J. Biol. Chem.* **284,** 792–798
11. Sheng, S., Bruns, J. B., and Kleyman, T. R. (2004) Extracellular histidine residues crucial for Na^+ self-inhibition of epithelial Na^+ channels. *J. Biol. Chem.* **279,** 9743–9749
12. Sheng, S., Carattino, M. D., Bruns, J. B., Hughey, R. P., and Kleyman, T. R. (2006) Furin cleavage activates the epithelial Na^+ channel by relieving Na^+ self-inhibition. *Am. J. Physiol. Renal Physiol.* **290,** F1488–F1496
13. Maarouf, A. B., Sheng, N., Chen, J., Winarski, K. L., Okumura, S., Carattino, M. D., Boyd, C. R., Kleyman, T. R., and Sheng, S. (2009) Novel determinants of epithelial sodium channel gating within extracellular thumb domains. *J. Biol. Chem.* **284,** 7756–7765
14. Anantharam, A., Tian, Y., and Palmer, L. G. (2006) Open probability of the epithelial sodium channel is regulated by intracellular sodium. *J. Physiol.* **574,** 333–347
15. Kellenberger, S., Gautschi, I., Rossier, B. C., and Schild, L. (1998) Mutations causing Liddle syndrome reduce sodium-dependent downregulation of the epithelial sodium channel in the *Xenopus* oocyte expression system. *J. Clin. Invest.* **101,** 2741–2750
16. Jasti, J., Furukawa, H., Gonzales, E. B., and Gouaux, E. (2007) Structure of acid-sensing ion channel 1 at 1.9 Å resolution and low pH. *Nature* **449,** 316–323
17. Liechti, L. A., Bernèche, S., Bargeton, B., Iwaszkiewicz, J., Roy, S., Michielin, O., and Kellenberger, S. (2010) A combined computational and functional approach identifies new residues involved in pH-dependent gating of ASIC1a. *J. Biol. Chem.* **285,** 16315–16329
18. Paukert, M., Chen, X., Polleichtner, G., Schindelin, H., and Gründer, S. (2008) Candidate amino acids involved in H^+ gating of acid-sensing ion channel 1a. *J. Biol. Chem.* **283,** 572–581
19. Krauson, A. J., Rued, A. C., and Carattino, M. D. (2013) Independent contribution of extracellular proton binding sites to ASIC1a activation. *J. Biol. Chem.* **288,** 34375–34383
20. Hughey, R. P., Bruns, J. B., Kinlough, C. L., Harkleroad, K. L., Tong, Q.,

Carattino, M. D., Johnson, J. P., Stockand, J. D., and Kleyman, T. R. (2004) Epithelial sodium channels are activated by furin-dependent proteolysis. *J. Biol. Chem.* **279,** 18111–18114
21. Hughey, R. P., Bruns, J. B., Kinlough, C. L., and Kleyman, T. R. (2004) Distinct pools of epithelial sodium channels are expressed at the plasma membrane. *J. Biol. Chem.* **279,** 48491–48494
22. Bruns, J. B., Carattino, M. D., Sheng, S., Maarouf, A. B., Weisz, O. A., Pilewski, J. M., Hughey, R. P., and Kleyman, T. R. (2007) Epithelial Na^+ channels are fully activated by furin- and prostasin-dependent release of an inhibitory peptide from the g-subunit. *J. Biol. Chem.* **282,** 6153–6160
23. Carattino, M. D., Sheng, S., Bruns, J. B., Pilewski, J. M., Hughey, R. P., and Kleyman, T. R. (2006) The epithelial Na^+ channel is inhibited by a peptide derived from proteolytic processing of its a subunit. *J. Biol. Chem.* **281,** 18901–18907
24. Kashlan, O. B., Adelman, J. L., Okumura, S., Blobner, B. M., Zuzek, Z., Hughey, R. P., Kleyman, T. R., and Grabe, M. (2011) Constraint-based, homology model of the extracellular domain of the epithelial Na^+ channel a subunit reveals a mechanism of channel activation by proteases. *J. Biol. Chem.* **286,** 649–660
25. Kashlan, O. B., Boyd, C. R., Argyropoulos, C., Okumura, S., Hughey, R. P., Grabe, M., and Kleyman, T. R. (2010) Allosteric inhibition of the epithelial Na^+ channel (ENaC) through peptide binding at peripheral finger and thumb domains. *J. Biol. Chem.* **285,** 35216–35223
26. Kashlan, O. B., Blobner, B. M., Zuzek, Z., Carattino, M. D., and Kleyman, T. R. (2012) Inhibitory tract traps the epithelial Na^+ channel in a low activity conformation. *J. Biol. Chem.* **287,** 20720–20726
27. Kellenberger, S., Gautschi, I., and Schild, L. (1999) A single point mutation in the pore region of the epithelial Na^+ channel changes ion selectivity by modifying molecular sieving. *Proc. Natl. Acad. Sci. U.S.A.* **96,** 4170–4175
28. Collier, D. M., Peterson, Z. J., Blokhin, I. O., Benson, C. J., and Snyder, P. M. (2012) Identification of extracellular domain residues required for epithelial Na^+ channel activation by acidic pH. *J. Biol. Chem.* **287,** 40907–40914
29. Chraïbi, A., and Horisberger, J. D. (2002) Na self inhibition of human epithelial Na channel: temperature dependence and effect of extracellular proteases. *J. Gen. Physiol.* **120,** 133–145
30. Ishikawa, T., Marunaka, Y., and Rotin, D. (1998) Electrophysiological characterization of the rat epithelial Na^+ channel (rENaC) expressed in MDCK cells: effects of Na^+ and Ca^{2+}. *J. Gen. Physiol.* **111,** 825–846
31. Collier, D. M., and Snyder, P. M. (2011) Identification of epithelial Na^+ channel (ENaC) intersubunit Cl^- inhibitory residues suggests a trimeric agb channel architecture. *J. Biol. Chem.* **286,** 6027–6032
32. Chen, J., Myerburg, M. M., Passero, C. J., Winarski, K. L., and Sheng, S. (2011) External Cu^{2+} inhibits human epithelial Na^+ channels by binding at a subunit interface of extracellular domains. *J. Biol. Chem.* **286,** 27436–27446
33. Rauh, R., Diakov, A., Tzschoppe, A., Korbmacher, J., Azad, A. K., Cuppens, H., Cassiman, J. J., Dötsch, J., Sticht, H., and Korbmacher, C. (2010) A mutation of the epithelial sodium channel associated with atypical cystic fibrosis increases channel open probability and reduces Na^+ self inhibition. *J. Physiol.* **588,** 1211–1225
34. Horisberger, J. D., and Chraïbi, A. (2004) Epithelial sodium channel: a ligand-gated channel? *Nephron Physiol.* **96,** p37–p41
35. Chen, J., Kleyman, T. R., and Sheng, S. (2013) Gain-of-function variant of the human epithelial sodium channel. *Am. J. Physiol. Renal Physiol.* **304,** F207–F213
36. Sheng, S., Maarouf, A. B., Bruns, J. B., Hughey, R. P., and Kleyman, T. R. (2007) Functional role of extracellular loop cysteine residues of the epithelial Na^+ channel in Na^+ self-inhibition. *J. Biol. Chem.* **282,** 20180–20190
37. Edelheit, O., Hanukoglu, I., Dascal, N., and Hanukoglu, A. (2011) Identification of the roles of conserved charged residues in the extracellular domain of an epithelial sodium channel (ENaC) subunit by alanine mutagenesis. *Am. J. Physiol. Renal Physiol.* **300,** F887–F897
38. Winarski, K. L., Sheng, N., Chen, J., Kleyman, T. R., and Sheng, S. (2010) Extracellular allosteric regulatory subdomain within the g subunit of the epithelial Na^+ channel. *J. Biol. Chem.* **285,** 26088–26096
39. Edelheit, O., Ben-Shahar, R., Dascal, N., Hanukoglu, A., and Hanukoglu, I. (2014) Conserved charged residues at the surface and interface of epithelial sodium channel subunits-roles in cell surface expression and the sodium self-inhibition response. *FEBS J.* **281,** 2097–2111
40. Condliffe, S. B., Zhang, H., and Frizzell, R. A. (2004) Syntaxin 1A regulates ENaC channel activity. *J. Biol. Chem.* **279,** 10085–10092
41. Sheng, S., Perry, C. J., and Kleyman, T. R. (2004) Extracellular Zn^{2+} activates epithelial Na^+ channels by eliminating Na^+ self-inhibition. *J. Biol. Chem.* **279,** 31687–31696
42. Collier, D. M., and Snyder, P. M. (2009) Extracellular chloride regulates the epithelial sodium channel. *J. Biol. Chem.* **284,** 29320–29325
43. Liu, W., Chun, E., Thompson, A. A., Chubukov, P., Xu, F., Katritch, V., Han, G. W., Roth, C. B., Heitman, L. H., Ijzerman, A. P., Cherezov, V., and Stevens, R. C. (2012) Structural basis for allosteric regulation of GPCRs by sodium ions. *Science* **337,** 232–236
44. Whorton, M. R., and MacKinnon, R. (2013) X-ray structure of the mammalian GIRK2-$\beta\gamma$ G-protein complex. *Nature* **498,** 190–197
45. Harding, M. M. (2002) Metal-ligand geometry relevant to proteins and in proteins: sodium and potassium. *Acta Crystallogr. D Biol. Crystallogr.* **58,** 872–874
46. Ji, H. L., Su, X. F., Kedar, S., Li, J., Barbry, P., Smith, P. R., Matalon, S., and Benos, D. J. (2006) δ-Subunit confers novel biophysical features to $\alpha\ \beta\ \gamma$-human epithelial sodium channel (ENaC) via a physical interaction. *J. Biol. Chem.* **281,** 8233–8241
47. Baconguis, I., and Gouaux, E. (2012) Structural plasticity and dynamic selectivity of acid-sensing ion channel-spider toxin complexes. *Nature* **489,** 400–405